A Novel Reconfigurable Metal Rim Integrated Open Slot Antenna for Octa-band Smartphone Applications

Manoj Stanley, Yi Huang, *Senior Member, IEEE,* Hanyang Wang, *Senior Member, IEEE*, Hai Zhou, Zhihao Tian and Qian Xu

***Abstract*— In this paper, a novel reconfigurable open slot antenna has been proposed for LTE smartphone applications to cover a wide bandwidth of 698-960 MHz and 1710-2690 MHz. The antenna is located at the bottom portion of the mobile phone and is integrated with metal rim, thereby occupying a small space and providing mechanical stability to the mobile phone. Varactor diode is used to cover the lower band frequencies, so as to achieve a good frequency coverage and antenna miniaturization. The operational principles of the antenna are studied and the final design is optimized, fabricated and tested. It has achieved the desired impedance bandwidth and the total efficiency of minimum 50% in free space throughout the required bands. The antenna performance with mobile phone components and human hand is also been studied. Furthermore, the SAR in a human head is investigated and is found to be within allowable SAR limits. Finally a Multiple Input-Multiple-Output antenna configuration with high isolation is proposed; it has an identical reconfigurable open slot antenna integrated at the top edge of the mobile phone acting as the secondary antenna for 698-960 MHz and 1710-2690 MHz. Thus the proposed antenna is an excellent candidate for LTE smart phones and mobile devices.**

***Index Terms*— LTE/WWAN antenna, metal rim, MIMO, open slot antenna, reconfigurable antenna, SAR, total efficiency.**

I. Introduction

In recent years, many wireless communication systems for different working frequencies and communication protocols have been developed and deployed worldwide. To provide all these services, the antenna in mobile phones should cover multiple frequency bands. In addition, since a large display with a narrow frame has become the mainstream of the modern mobile phones, the space for antennas is very limited. So, designing a multiband/wideband mobile antenna with a small size is not only an essential requirement but also a major technological challenge. The antenna must be capable of covering 698-960 MHz and 1710-2690 MHz which covers the LTE700, GSM850, GSM900, GSM1800, GSM1900, UMTS, LTE2300, and LTE2500 bands. Also the antenna must achieve minimum 50% total efficiency throughout these bands. Many interesting designs have been developed by researchers using different design principles. In the past two decades, there has been a wealth of publications on internal antenna innovations for mobile handset antennas, e.g. single-band PIFAs [1], [2], dual-band PIFAs [3], capacitive loading [4], shorting techniques [5], capacitive feeding [6], parasitic elements [7], combinations of different loading techniques [8], resonant slots [9], [10], loop antennas[11] and active antennas [14].

A smartphone with a metal rim has also become attractive since the metal rim increase the mechanical strength of the mobile phone and enhances its aesthetic appearance. The performance of the traditional internal antennas such as PIFA, monopole, loop, etc. will be adversely affected, if the metal rim is not modified accordingly, making it difficult to achieve wideband performance [15], [16]. Many approaches have been tried before to integrate metal rim in mobile phones. In one of the approaches, multiple gaps and grounded patches were inserted to minimize metal rim effect [16]. The position of the gaps and the patches were carefully chosen. The disadvantage of this approach is that by creating multiple gaps in the metal frame, the mechanical stability is compromised. Also internal antenna used in this approach, at the bottom side of the mobile phone consumes a lot of space. Two slots were introduced in the metal rim in [12] and [13] to create resonances to cover the lower band. The presence of the slots compromise the performance in the presence of the user's hand. In another approach, a slot antenna of 15.5 × 56.5 mm^2 was introduced in the bottom of the system ground [17]. The slot was fed by a feeding strip and the antenna could cover GSM850/900/DCS/PCS/UMTS2100 operation. This was not a wide band solution and was not capable of covering the entire 698-960 MHz and 1710-2690 MHz. In another design, IFA structure together with slot in the ground plane was used to cover GSM850/900/DCS/PCS/UMTS2100/LTE2300/2500 operating bands [18]. The bandwidth of the lower band was not wide enough to cover LTE700 and multi-antenna configuration is not possible for the low band. In another open slot design for laptop applications, two separate feeds were used to excite the antenna [19]. Open-slot antennas that have been reported for tablet computers [20], [21] have a large ground clearance which is not suitable for modern mobile phones. In another recently

The work is supported by Huawei Technologies, Shenzhen, China.

M. Stanley, Y. Huang (corresponding author), Z. Tian and Q Xu are with the Department of Electrical Engineering and Electronics, The University of Liverpool, Liverpool, L69 3GJ, United Kingdom (e-mail: manoj.stanley@liv.ac.uk; yi.huang@liv.ac.uk; zhihao.tian@liv.ac.uk; qian.xu@liv.ac.uk).

H. Y. Wang and H. Zhou are with Huawei Technology (UK) Co. Ltd, Reading, RG2 6UF, United Kingdom (email: hanyang.wang@huawei.com; hai.zhou1@huawei.com).

This article has been accepted for publication in a future issue of this journal, but has not been fully edited. Content may change prior to final publication. Citation information: DOI 10.1109/TAP.2017.2700084, IEEE Transactions on Antennas and Propagation

published design, a PIN diode was used to perform reconfiguration by switching states [22]. This is a very promising design, but covers only a part of the lower band.

It is definitely challenging to design a multiband/wideband antenna for a metal-rim integrated smartphone, due to the complicated frame structure. To alleviate these problems, a reconfigurable open slot antenna fed by an L-shaped micro-strip feed line capable of supporting octa-band operations is proposed. The open slot antenna can achieve miniaturization by exciting its fundamental mode. Furthermore, the slot can be easily integrated with the metal rim. The greatest achievement is that the proposed antenna can be used for multi-antenna implementation to cover both the lower band and higher band with a very low correlation between the antennas. The proposed antenna has a clearance size of 11 mm, which is favorable for modern smartphones. A varactor diode is used for reconfiguration, resulting in multiple states. As a result, the reconfigurable open slot antenna covers the entire 698-960 MHz and 1710-2690 MHz.

In Section II, the proposed antenna configuration and operation principle are explained. Some important design parameters are investigated in detail in Section III. The total efficiency, reflection coefficient are shown in Section IV. The effect of user's hand, effect of mobile phone components and the SAR values are also studied. Performance of the proposed antenna with recent antenna designs is also investigated. In Section V, the implementation of multi-antenna configuration with high isolation is proposed. Some conclusions are given in Section VI indicating the achievements of this research.

II. ANTENNA CONFIGURATION AND PRINCIPLE OF OPERATION

A. Antenna Configuration

In this section, the reconfigurable open slot antenna design is introduced. Fig. 1(a) shows the geometry of the proposed antenna for LTE/WWAN metal-rimmed smartphones, whose detailed structure and optimized dimensions are shown in Fig. 1(b). As illustrated in Fig. 1(a), a 0.8-mm thick FR4 substrate of relative permittivity 4.4 and loss tangent 0.02 is used as the system circuit board of size 150 × 74 mm^2. It is surrounded by a metal rim of height 7 mm and thickness of 1 mm. There is no gap between the PCB and the metal rim, which in turn increases the mechanical strength of the system. A ground plane of size 130 × 74 mm^2 serves as the smartphone's ground plane. The design shown in Fig. 1(a) has an inverted unsymmetrical T-shaped wide slot cut on the system circuit board. The slot also opens the metal rim which is connected to the ground plane.

As shown in Fig. 1(b), the proposed reconfigurable open slot antenna mainly contains an L-shaped feed strip at the opposite side of the FR4 substrate, a varactor diode branch and a gap at the top portion of the metal rim. A 50-Ω SMA connector is soldered to feed the antenna (point *F*). A branch with a variable capacitor/varactor diode added to the back side of the feed strip can be used to tune the entire lower band. Varactor diode needs appropriate biasing for its operation. The PCB is positioned at the center of metal rim as shown in Fig. 1(c).

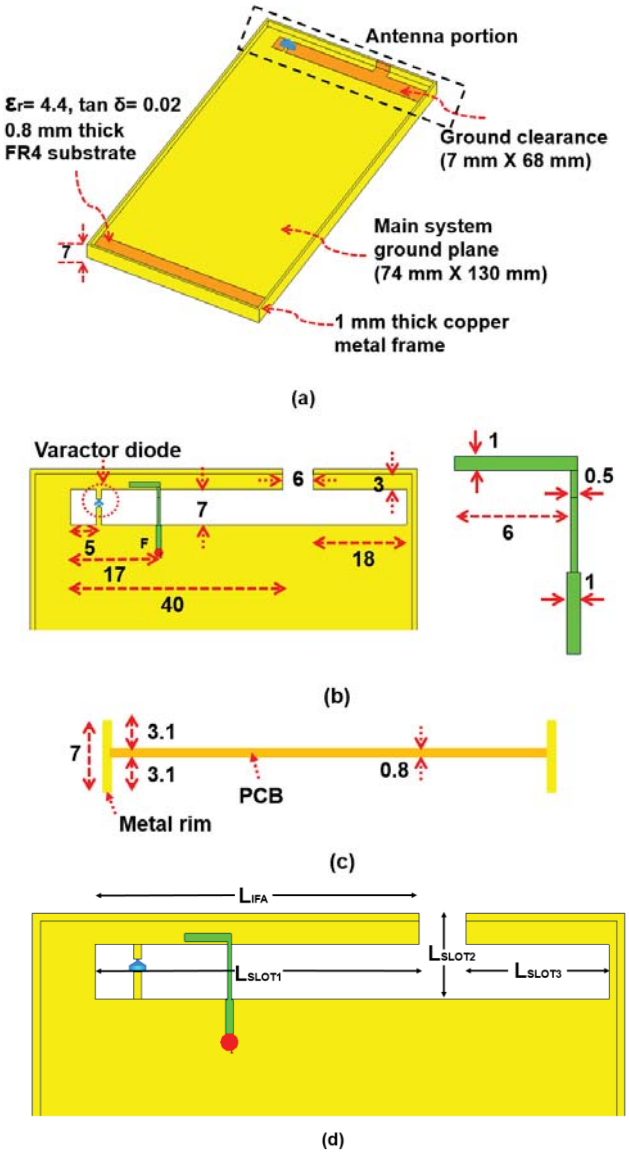

Fig. 1 Proposed reconfigurable narrow-frame antenna configuration (Unit: mm): (a) Geometry of the metal-rimmed antenna; (b) Detailed dimensions of the pro-posed antenna and micro-strip feed (c) Position of PCB. (d) Zoomed antenna portion with annotation.

A major portion of the metal rim is shorted to the ground plane, thereby increasing the mechanical stability. The open slot in the metal rim is filled with FR4 to enhance structural rigidity. The slot enclosed by the metal rim with a gap of 6 mm is excited by the L-shaped strip. There is only one resonant mode in the lower band. There are two resonances in the higher band. The feeding strip introduces a capacitive loading. All three resonances can be controlled by changing the length of the feeding strip. The resonant frequency in the lower band is decided by the slot length of L_{SLOT1}+L_{SLOT2} which is 50 mm, as shown in Fig. 1(d) thereby, creating an open slot antenna resonating at about 0.92 GHz in free space (0.16λ). There are two resonant frequencies in the higher band. One is around 1.54 GHz due to the L_{IFA} which is 42 mm, thereby, creating an IFA mode around 0.25λ. The other resonance around 2.5 GHz is due

This article has been accepted for publication in a future issue of this journal, but has not been fully edited. Content may change prior to final publication. Citation information: DOI 10.1109/TAP.2017.2700084, IEEE Transactions on Antennas and Propagation

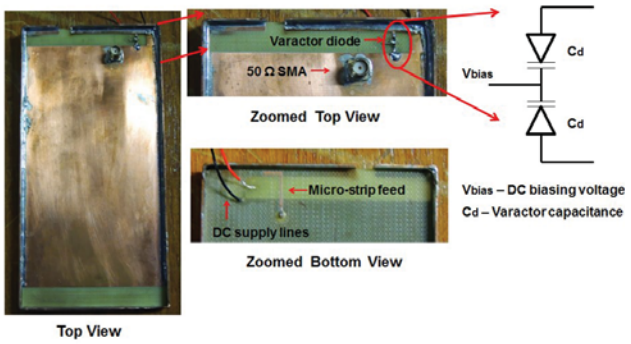

Fig. 2. Fabricated reconfigurable open slot antenna.

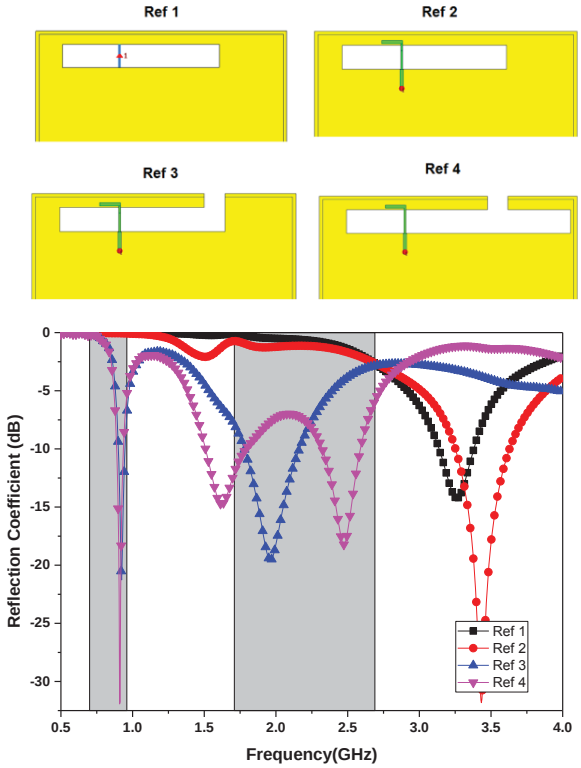

Fig. 3. Simulated reflection coefficients results for reference antennas.

to L_{SLOT2}+L_{SLOT3} which is around 28 mm, creating an open slot antenna resonating at 0.25λ.

The proposed reconfigurable open slot antenna was fabricated and tested to prove the operation. The fabricated antenna with biasing topology for varactor diode is shown in Fig. 2. The slot is filled with FR4 in the mockup, but not shown in Fig. 2. Two varactor diodes are arranged in series in back to back configuration. The back-to-back configuration overcomes the problem of the RF modulating the tuning voltage as the effect is cancelled out. As the RF voltage rises, the capacitance on one diode will increase and the other diode will decrease. The back-to-back configuration also halves the capacitance of the single diode as the capacitances from the two diodes are placed in series with each other. Hence the equivalent varactor diode capacitance of this configuration is $C_d/2$. The varactor

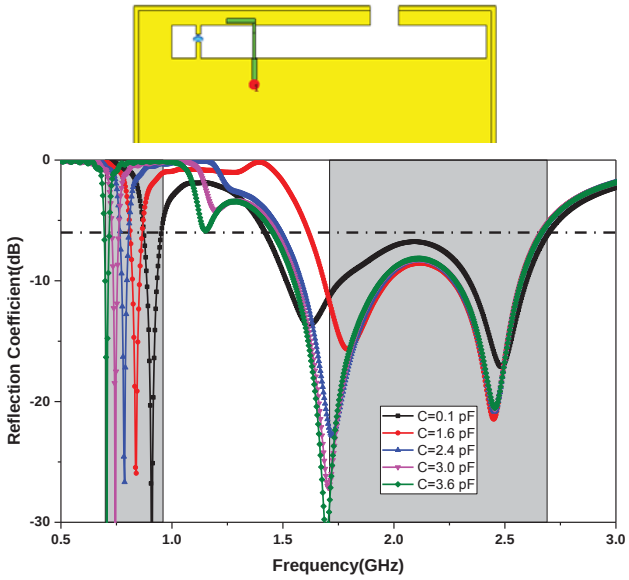

Fig. 4. Simulated reflection coefficients results of proposed antenna for different values of varactor diode capacitance.

diode used for fabrication is Infineon BB857-02V H7902. The DC voltage is fed directly to the varactor diode and varied from 1-30V. The minimum achievable equivalent varactor diode capacitance is 0.4 pF and maximum achievable equivalent varactor diode capacitance is 3 pF. These values are not sufficient to cover the required tuning range, but enough to prove the working principle. The principle of using a variable capacitor has been demonstrated using a varactor diode in this work. There are other solutions such as a digitally tuned capacitor (DTC), which uses a lower supply voltage and can be programmed. Another option is to use switching of set of fixed capacitors to achieve reconfiguration which is employed in several adaptive matching circuits in commercial devices.

B. Principle of Operation

The working principle can be clearly understood by using four reference antenna designs. A simple version of the proposed antenna without the varactor diode branch is initially considered. It is well known that closed slot antenna resonates at 0.5λ. But if the same slot is opened, the antenna resonates at 0.25λ instead of 0.5λ, which leads in size reduction. The loading effect due to FR4 substrate has reduced the slot antenna resonance to 0.16λ.

As seen in Fig. 3, Ref 1 shows a closed slot antenna with perimeter of 84 mm cut in the system ground plane and excited using a direct feed. The antenna is expected to resonate at a frequency around 3.5 GHz owing to 0.5λ slot mode which is verified by simulation. In Ref 2 the closed slot antenna is fed by an L-shaped feeding strip. A resonance is observed around 1.5 GHz due to the introduction of a capacitive feeding strip. However the impedance matching of this resonance is poor. Now a slot is introduced in the metal frame with the slot perimeter almost kept the same as shown in Ref 3 in Fig. 3. There are two resonant frequencies at 0.92 GHz and 1.8 GHz as

This article has been accepted for publication in a future issue of this journal, but has not been fully edited. Content may change prior to final publication. Citation information: DOI 10.1109/TAP.2017.2700084, IEEE Transactions on Antennas and Propagation

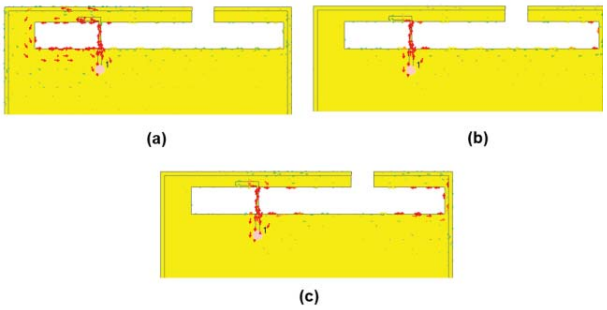

Fig. 5. Current distribution at frequencies: (a) 0.92 GHz; (b) 1.54 GHz; (c) 2.5 GHz

seen in the reflection coefficient result in Fig. 3. These are due to 0.16λ slot mode and 0.25λ IFA mode respectively. Hence the introduction of the slot has created a resonant frequency in the low band of operation. In Ref 4 as shown in Fig. 3, we keep the slot in the metal rim and further increase the slot length in the ground plane. An additional resonance is created at 2.54 GHz due to 0.25λ slot mode. The resonance in the low band is unaffected as the extra slot length to the right of feed line adds no contribution to the 0.16λ slot mode. The design of Ref 4 is capable of covering six bands. Now the varactor diode branch is introduced in the design. The introduction of varactor diode branch will make it possible to tune the narrow bandwidth low band resonant frequency by varying the varactor diode capacitance. The varactor diode capacitance is varied by varying the bias voltage. This tuning capability makes the antenna reconfigurable and enables the proposed antenna to cover the eight bands frequency bands LTE700/GSM850/900/DCS/PCS/UMTS2100/LTE2300/2500. Simulated reflection coefficients results of proposed antenna for various values of varactor diode capacitance are shown in Fig. 4.

The current distribution of the antenna without varactor branch (Ref 3) at resonant frequencies is shown in Fig 5. The feed branch has strong currents in all the three resonant frequencies. At 0.92 GHz, currents are concentrated around the slot at the left. At 1.54 GHz, the currents are concentrated at the feed strip. At 2.5 GHz, currents are concentrated at the right end of the open slot.

The proposed antenna has three forms of capacitive loading which are created by the capacitive feed, the varactor diode and the rim slot size. The location and length of capacitive feed decide the capacitive loading created by the feeding. As the length of the capacitive feed increases, the capacitance loading also increases which decreases the three resonant frequencies. The capacitive loading from varactor diode only affects the low band frequency as seen from the return loss plot in Fig.4. As the capacitance associated with the varactor diode increases, the resonant frequency decreases. By varying the rim-slot gap, the first and third resonant frequency can be fine-tuned. It also affects the impedance matching of the second resonant frequency as seen in Fig. 9. As the rim-slot gap increases, the capacitive loading associated with the rim-slot gap decreases and hence the first and third resonant frequencies increase.

The design equations for antenna design have been formulated neglecting the capacitive loading to keep the

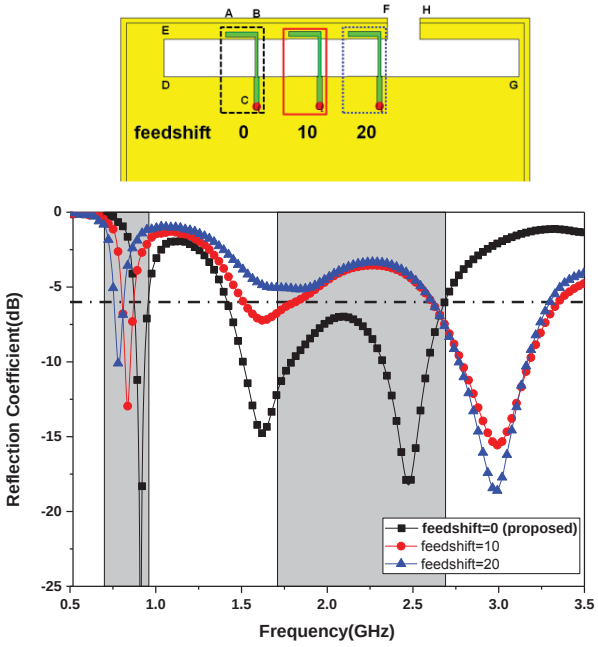

Fig. 6. Effect of feeding strip location on antenna performance.

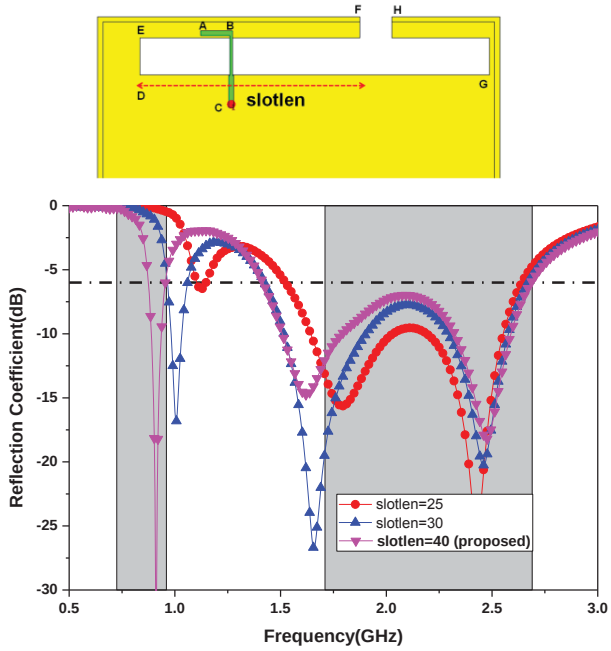

Fig. 7. Effect of length of slot on antenna performance.

understanding simple. The initial lengths could be set as per the given equations. The markings are shown in Fig. 1(d).

$$L_{SLOT1} + L_{SLOT2} = 0.16\lambda_1 \quad (1)$$

$$L_{IFA} = 0.25\lambda_2 \quad (2)$$

$$L_{SLOT2} + L_{SLOT3} = 0.25\lambda_3 \quad (3)$$

where λ_1, λ_2 and λ_3 are wavelengths corresponding to resonant frequencies 0.92 GHz, 1.54 GHz and 2.5 GHz respectively.

This could be followed by a parametric based optimization to determine the precise final dimensions.

This article has been accepted for publication in a future issue of this journal, but has not been fully edited. Content may change prior to final publication. Citation information: DOI 10.1109/TAP.2017.2700084, IEEE Transactions on Antennas and Propagation

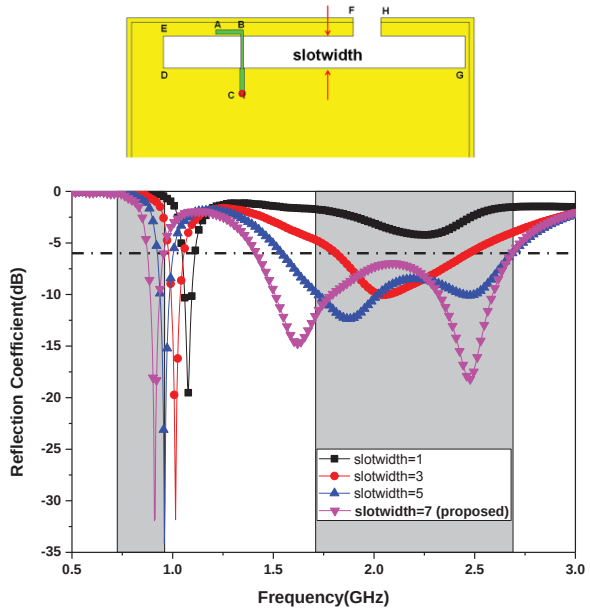

Fig. 8. Effect of width of slot on ground plane on antenna performance.

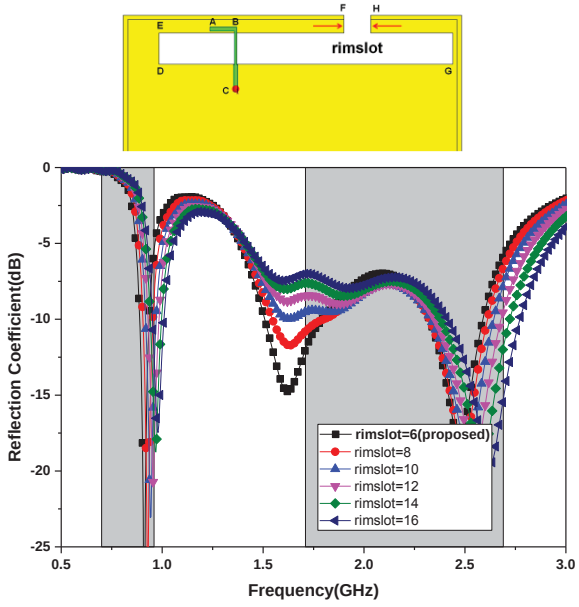

Fig. 9. Effect of size of slot on metal rim on antenna performance.

III. DESIGN PARAMETRIC STUDY

It is necessary to understand how the design parameters affect antenna performance. To optimize the antenna performance, some important design parameters and their effects are to be studied. The analysis of these parameters is made without considering the varactor diode branch.

A. *Effect of feed position*

Fig. 6 shows the effect of varying feeding strip location. As seen from the current distribution at resonant frequencies, changing the feeding location affects the lower band resonant frequency due to capacitance loading. As the feed strip is shifted towards right, the resonant frequencies in the lower band decrease. The impedance matching of second resonant

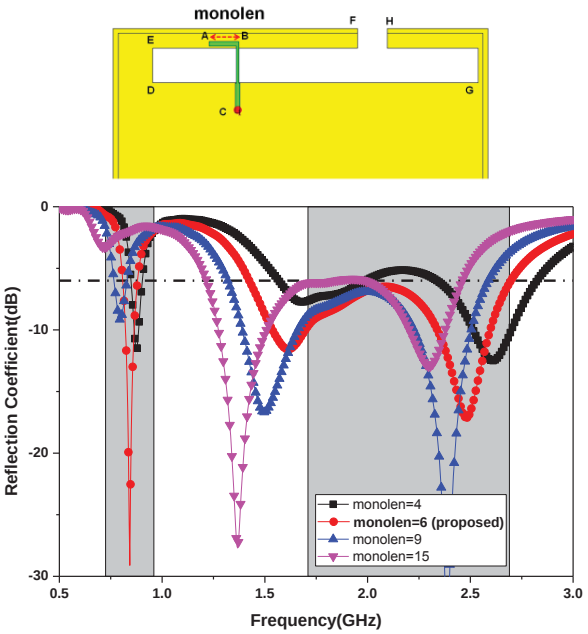

Fig. 10. Effect of length of feeding strip on antenna performance.

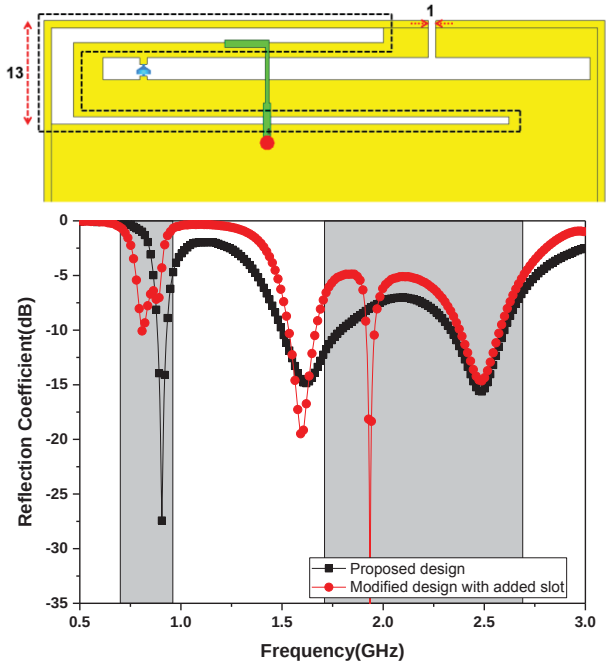

Fig. 11. Modified design with additional slot and performance comparison when C=0.1 pF.

frequency due to IFA mode depends on the location of the feed strip. As the feed strip is shifted left towards the short, the impedance matching is improved. As the feed strip is shifted towards the open end, impedance matching is deteriorated. This is in accordance with the IFA principle.

B. *Effect of slot length*

Fig. 7 shows the simulated reflection coefficient of the reference antenna as a function of the length of the slot in the ground plane which is present to the left of the metal rim slot. As the slot length is reduced, low band resonant frequency increases as expected due to reduction in L_{SLOT1}. There is no

This article has been accepted for publication in a future issue of this journal, but has not been fully edited. Content may change prior to final publication. Citation information: DOI 10.1109/TAP.2017.2700084, IEEE Transactions on Antennas and Propagation

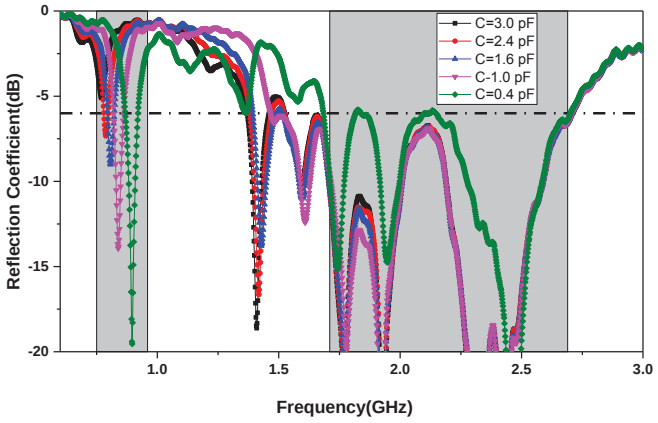

Fig. 12. Measured S-parameter of proposed antenna for different values of varactor diode capacitance.

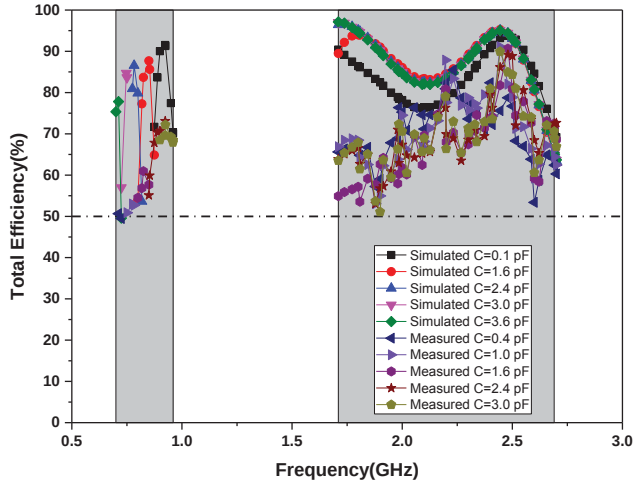

Fig. 13. Total efficiency of proposed antenna in free space for different values of varactor diode capacitance.

significant change in high band frequencies.

C. *Effect of slot width*

The variation in reflection coefficient of the reference antenna with the width of the slot is shown in Fig. 8. Slot width is an important parameter as this decides the required ground clearance area. As the width of the slot is increased, impedance matching improves in the higher band. In the low band, resonant frequency slightly lowers with increase in slot width. This is because section $\overline{DE}$ increases slightly increasing the perimeter of the slot. In the high band, the resonance due to 0.25λ IFA mode shifts downwards due to loading effect. The slot width should be a fraction of the wavelength at 1.54 GHz to maintain good impedance matching.

D. *Effect of rim cut size*

Another important parameter is the size of the slot cut on the metal rim. A capacitance exists in the metal rim gap. This capacitance will block the low frequencies. The size of the gap controls the capacitance which decreases as the gap size increases [20]. According to [19], the resonant frequency can be written as:

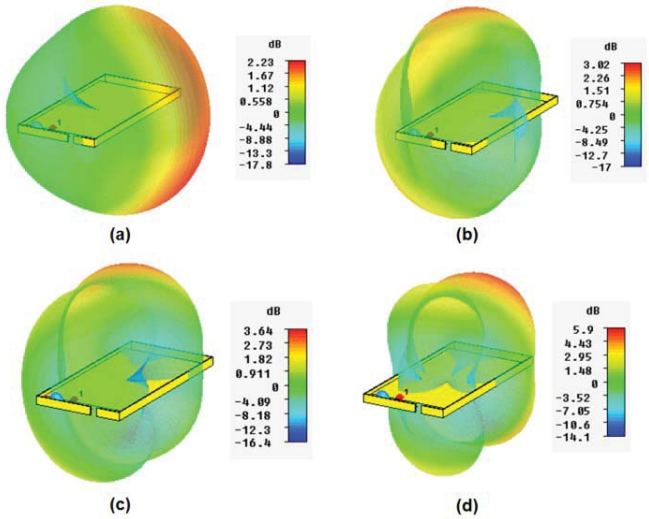

Fig. 14. 3-D far field gain pattern when varactor diode capacitance, C=0.1 pF: (a) 0.925 GHz; (b) 1.8 GHz; (c) 2.1 GHz; (d) 2.5GHz.

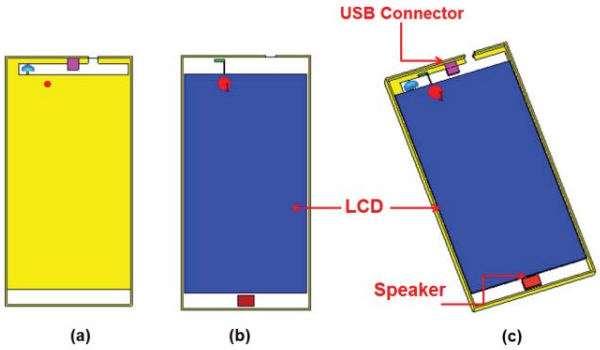

Fig. 15. Component placement study arrangement: (a) Top view; (b) Bottom view; (c) Perspective view

$$f_r = \frac{1}{2\pi\sqrt{L_{eff}C_{eff}}} \quad (4)$$

where f_r is the resonant frequency of the antenna, L_{eff} is the effective inductance and C_{eff} is the effective capacitance associated with the antenna.

Therefore, as the size of the rim slot increases, the lower band resonant frequency increases. Similarly, the resonance at the higher band due to 0.25λ IFA mode increases as the rim slot increases. Also, the bandwidth of the lower band is improved gradually as the size of the rim slot is increased. But for practical purpose, it is desired to keep the slot size as small as possible.

E. *Effect of length of feed strip*

The effect of the length of the L-shaped feeding strip is also analyzed. As the length of the feeding strip $\overline{AB}$ is increased, all the three resonant frequencies are lowered. This is due to the capacitive loading created by the feed. As the capacitance loading increases, the resonant frequency decreases.

F. *Effect of additional slot*

An additional slot as indicated by black dashed lines in Fig. 11 has been added to the proposed design to improve the bandwidth in the lower band. The added slot operates in 0.5λ

This article has been accepted for publication in a future issue of this journal, but has not been fully edited. Content may change prior to final publication. Citation information: DOI 10.1109/TAP.2017.2700084, IEEE Transactions on Antennas and Propagation

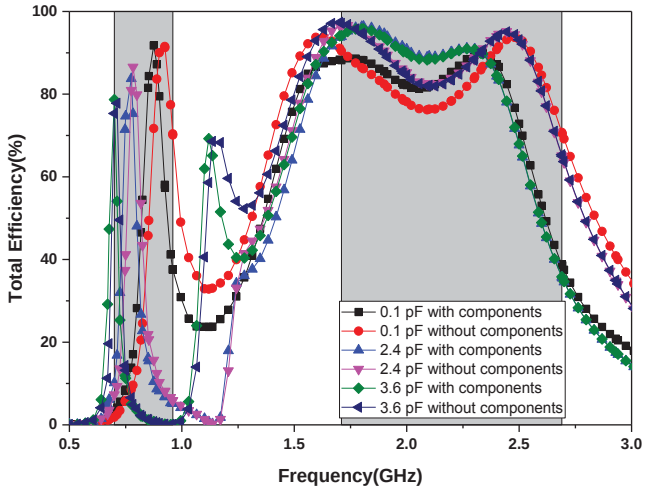

Fig. 16. Simulated total efficiency of the proposed antenna in the presence of components.

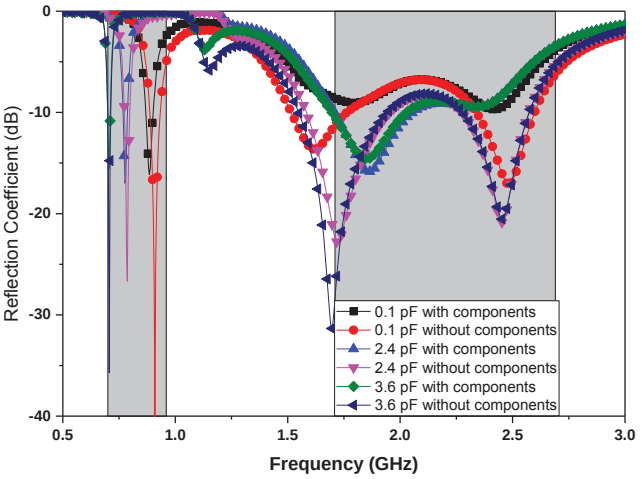

Fig. 17. Simulated reflection coefficients of the proposed antenna in the presence of components.

slot mode in the low band and generate 1λ higher mode in the higher band. The bandwidth in the lower band is improved by merging the 0.5λ slot mode generated by the added slot with the 0.16λ open slot mode. This modification also helps in reducing the rim cut size to 1 mm without compromising the antenna performance in the lower band as seen by the reflection coefficient result in Fig. 14. However, the ground clearance is increased to 13 mm in the modified design.

IV. PERFORMANCE EVALUATION

A. Free Space

The measured reflection coefficient results are shown in Fig. 12. There is coupling between the DC bias wires and the antenna resulting in additional resonances as seen in Fig. 12. It is possible to isolate the DC bias wires from RF signal by introducing DC blocking capacitance and RF choking inductor. However, the addition of two lumped components will further degrade the total efficiency. This also increases the cost of production. The varactor diode used for fabrication has possible values from 0.4 pF to 3 pF only. Hence the measured results

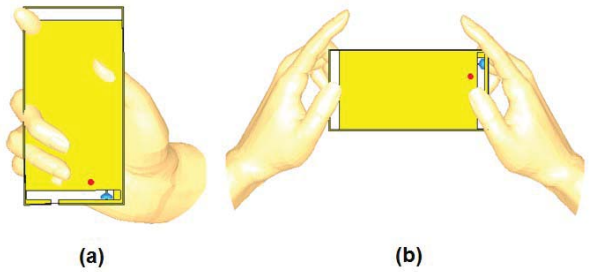

Fig. 18. Hand grip position: (a) One-hand talk mode; (b) Two-hand data mode.

show 6 dB return loss from 730 MHz-940 MHz in the lower band. The entire higher band has very good measured impedance matching.

Simulated and measured total efficiency for different values of varactor diode capacitance are shown in Fig. 13. In the simulation, the varactor diode is modelled as an ideal capacitor. But in reality there is an insertion loss in the varactor diode due to the non-ideal series resistance in the varactor diode. During

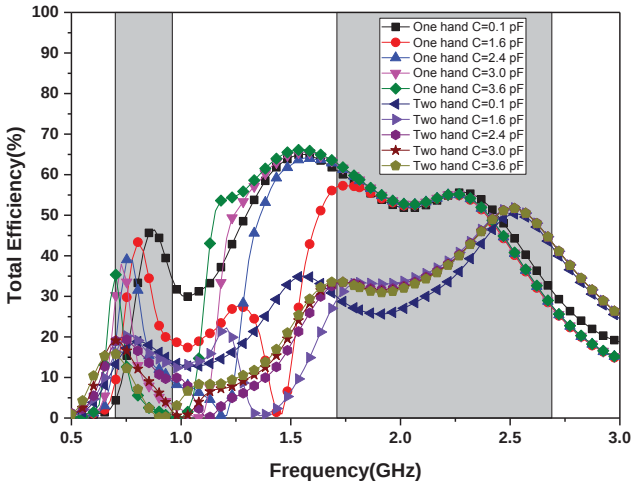

Fig. 19. Simulated total efficiency for hand grip position.

fabrication the variable capacitor is realized using two varactor diodes in series. By connecting them in series, the effective capacitance is halved, thereby providing capacitance as low as 0.4 pF. But the losses in the varactor diodes add up. Hence there is reduction in measured efficiency. Simulated 3D far field gain patterns are shown in Fig. 14 which are not symmetrical due to the asymmetrical antenna structure.

B. Effect of Components

Detailed analysis of effects of mobile phone components to antenna performance is shown in this section. To see the effect of components, a speaker of size 10 mm × 6 mm × 2.5 mm, standard 5 inch LCD screen and a USB connector of size 7 mm × 6.9 mm × 1.85 mm are placed in accordance with a standard mobile phone as shown in Fig. 15. A suitable position for USB connector is proposed so that the antenna performance is not affected. The USB connector is placed in the center of metal rim and connected to the ground plane and metal rim. Hence the USB connector is made as a part of the antenna. The speaker is placed in floating configuration and is not connected to the

This article has been accepted for publication in a future issue of this journal, but has not been fully edited. Content may change prior to final publication. Citation information: DOI 10.1109/TAP.2017.2700084, IEEE Transactions on Antennas and Propagation

TABLE I
SIMULATED SAR VALUES FOR 1-G HEAD TISSUE

Frequency (MHz)		750	825	900	1800	2250	2700
Input power (Watt in dBm)		24	24	24	21	21	21
1-g SAR (W/kg)	C=0.1 pF	0.23	0.34	0.51	0.36	0.33	0.65
	C=1.6 pF	0.23	0.54	0.27	0.42	0.39	0.64
	C=2.4 pF	0.46	0.58	0.10	0.41	0.38	0.64
	C=3 pF	0.59	0.14	0.04	0.41	0.37	0.64
	C=3.6 pF	0.34	0.05	0.01	0.41	0.37	0.64

metal rim. Simulated total efficiency of proposed antenna in the presence of components is shown in Fig. 16 and the simulated reflection coefficients are shown in Fig. 17. The results are simulated for some values of capacitance only to be concise. It can be seen that there is a slight offset in efficiency performance in the lower band due to the presence of the dielectric due to the LCD screen. There is reduction in total efficiency in the higher band due to the USB connector. The higher band performance can be further optimized by shifting the feeding strip.

C. *Effects of Hand*

The effects of the user's hand on antenna performances have been studied in [11], [25] and [26]. Building on previous work, this section investigates the performance of antenna in various standard hand grips. Fig. 18 shows the two investigated grip positions: one-hand grip at the top position of the handset which is the talk mode and two-hand mode or the data mode. The hand models are very similar to CTIA models used by the industry for performance evaluation [33]. Generally, the user hand reduces the antenna total efficiency and often degrades the impedance matching. The simulated total efficiency of the open slot antenna for one-hand grip at top position and two-hand data mode are shown in Fig. 19. When the user hand is in proximity to the antenna, efficiency will be deteriorated as expected. However, in one-hand talk mode, the efficiency reduction is not very high. All of these results have close agreements with data obtained in [25], [26].

The total efficiency reduction is significant in two-hand data mode which is as low as 18% in the low band. Also when the user hand covers the rim slot, the efficiency drops significantly to 6-10% in the low band and 6-18% in the high band. This issue can be solved by using diversity antennas and adaptive matching techniques. During such cases, a diversity antenna would prove to be very useful. Recent work is focused on developing adaptive impedance matching networks which could be another solution to reduce hand effects.

D. *SAR Performance*

The human head model used for SAR calculation and the calculated SAR values for 1-g head tissue are shown in Fig. 20 and Table I respectively, estimated using CST 2014. In the simulation, the gap between ear and the mobile is 1 mm and the gap between the mobile and cheek is around 8 mm which are quite close to practical scenarios. The input transmit power for

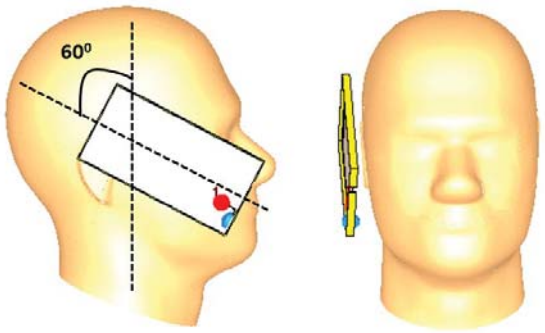

Fig. 20. Simulation model of SAR.

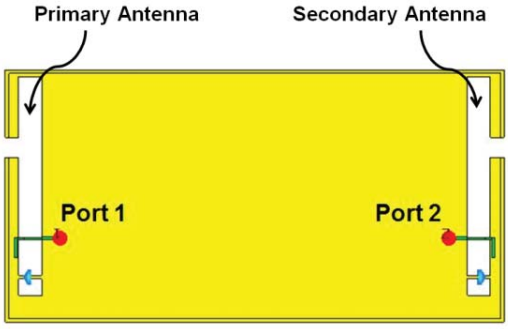

Fig. 21. Proposed MIMO configuration.

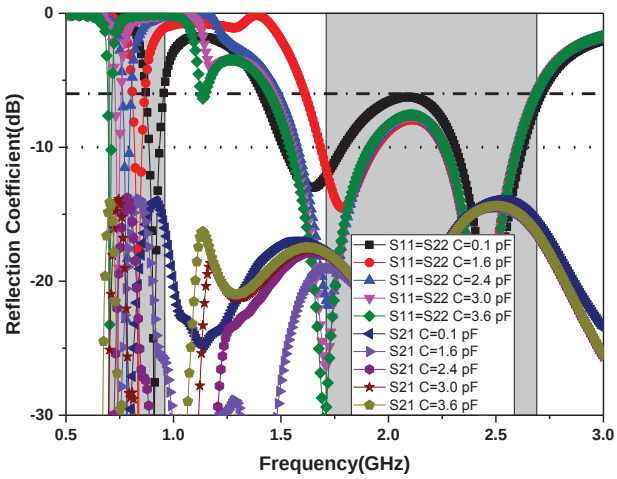

Fig. 22. Simulated reflection coefficients for the MIMO configuration.

SAR calculation is 24 dBm for lower band frequencies and 21 dBm for higher band frequencies and the calculated 1-g SAR are all listed in Table I. The calculated SAR values are well within the industry specified SAR limit of 1.6 W/kg for 1-g tissue.

E. *State-of-the-Art Comparison*

In order to evaluate the achievements of the proposed antenna with respect to available designs, the proposed antenna is compared with recently published designs. The key parameters were possible integration with metal rim, slots in the metal rim, size of the ground clearance, bandwidth and the total efficiency.

The proposed antenna exhibits a very low ground clearance yet exhibit a high bandwidth as opposed to other metal rim integrated designs. The proposed antenna could also be

This article has been accepted for publication in a future issue of this journal, but has not been fully edited. Content may change prior to final publication. Citation information: DOI 10.1109/TAP.2017.2700084, IEEE Transactions on Antennas and Propagation

TABLE II
COMPARISON OF PROPOSED ANTENNA PERFORMANCE WITH RECENT ANTENNA DESIGNS

Ref.	Proposed Antenna	[18]	[11]	[16]	[17]	[30]	[28]
Metal rim integration	**Yes**	Yes	Yes	Yes	Yes	No	No
Metal rim gaps	**Yes**	Yes	No	Yes	No	-	-
BW_{low} (MHz)	**698-960**	824-960	824-960	890-960	824-960	698-960	746-960
BW_{high} (MHz)	**1710-2690**	1710-2690	1710-2690	1710-2170	1710-2690	1630-2980	1700-2700
Ground clearance (mm)	**11**	9	11	16	9	16	12
Total efficiency in free space (%)	**50-95**	50-80	60-80	60-90	50-75	45-85	40-90
Total efficiency in presence of hand (%)	**30-60**	20-45	20-35	18-40	-	30-50	-
Possible MIMO configuration	**Yes**	No	No	No	No	Yes	Yes

BW_{low} = bandwidth at lower-band
BW_{high} = bandwidth at higher-band

implemented as a MIMO antenna for the lower band as well as the higher band which will be explained in the next section. This is a very good achievement for a metal rim integrated design. Therefore, the comparison indicates that the proposed antenna has very good performances with respect to bandwidth, miniaturization, total efficiency and possibility of MIMO.

V. MIMO IMPLEMENTATION

Multiple antennas help to multiply the capacity of a radio link and hence exploit multipath propagation [25]. It is very difficult to achieve high isolation between multiple antennas without properly designed and placed antennas. In [28], the frame was used as the antenna after adjusting the shorting pin location. But these structures will increase the complexity of the design and consume a lot of space. But the space inside a mobile phone is limited by the use of USB connectors, speaker, microphone, etc. A simple decoupling technique is to feed the secondary antenna in a suitable location on the ground plane using the diagonal modes. In [26], two collocated antennas were placed on the bottom edge of the PCB. But the bandwidth was very narrow. The design of multiple antennas can get very challenging at the lower bands as the chassis provides only single resonant mode at the lower frequencies. Hence additional resonant modes need to be created in order to design multiple antennas for the lower bands.

A multi-antenna system is implemented by placing a copy of the antenna on the top side of the system circuit board. The antennas are arranged to the same side of the circuit board as shown in Fig. 21, similar to a technique described in [30].

The simulated and measured reflection coefficients are shown in Fig. 22 and Fig. 23 respectively. For conciseness, the corresponding results of S_{22} are not shown in Fig. 22 and Fig.

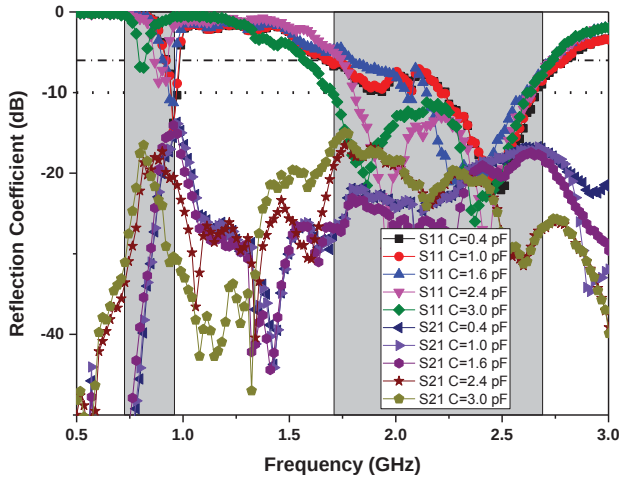

Fig. 23. Measured reflection coefficients for the proposed MIMO configuration.

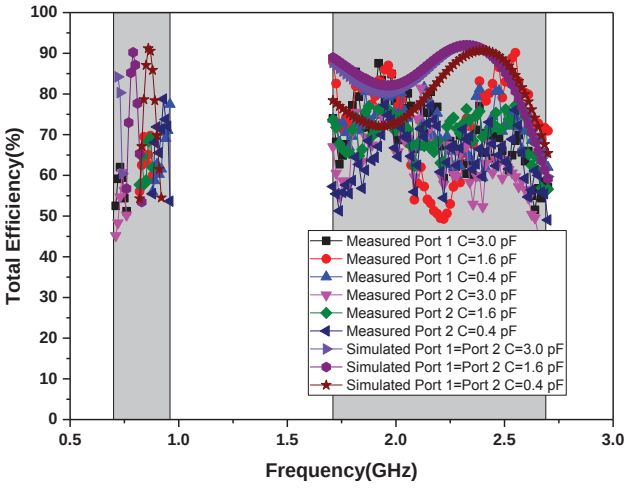

Fig. 24. Total efficiency for the proposed MIMO configuration.

This article has been accepted for publication in a future issue of this journal, but has not been fully edited. Content may change prior to final publication. Citation information: DOI 10.1109/TAP.2017.2700084, IEEE Transactions on Antennas and Propagation

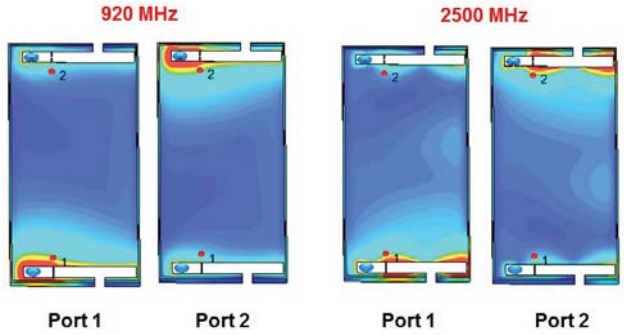

Fig. 25. Simulated surface current distribution for the MIMO configuration for the state when varactor diode capacitance is 0.1 pF.

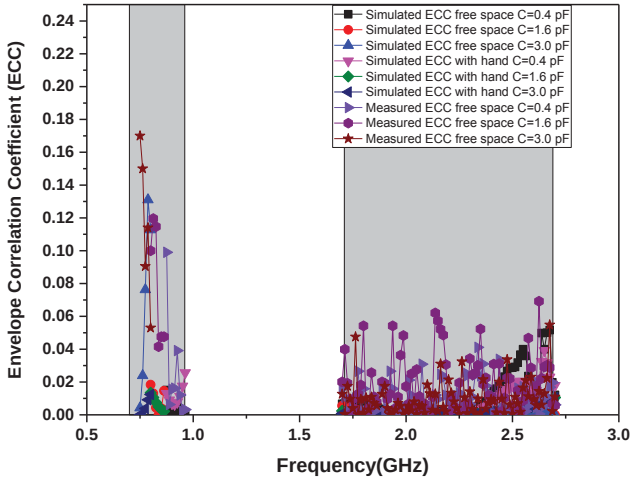

Fig. 26. Envelope Correlation Coefficient (ECC) for the proposed MIMO configuration.

23, as S_{11}=S_{22}. The worst case isolation of 14 dB has been achieved for the lower band which is better than any of the existing designs. Simulated and measured total efficiencies of the MIMO configuration are shown in Fig. 24.

Simulated current distributions at 0.92 GHz and 2.5 GHz when the varactor diode capacitance is 0.1 pF are shown in Fig.25. It is noted that Fig. 25 is observed when port 1 is excited while port 2 is terminated to a 50-Ω match load and vice-versa. It can be clearly seen that the induced current in port 2 is weaker for the lower band and higher band when port 1 is excited and vice-versa. The currents are localised around the slot in the ground plane even at lower frequencies. Hence the contribution of the system ground plane is very limited for radiation even at the lower band, unlike other antenna designs, where the ground plane plays a significant role for radiation in the lower band. Hence there is little coupling between the two antennas even though both the antennas share the same system ground plane. The disadvantage, however, is the narrow bandwidth in the lower band. But this issue has been solved by introducing the varactor diode, thereby providing the ability to tune the entire lower band.

The performance of multi-antennas has been examined using ECC (envelope correlation coefficient) which is considered as a suitable metric for evaluating MIMO antennas. The proposed MIMO configuration can satisfy required ECC. In the lower band, the simulated ECC in free space is less than 0.15 while in the higher band it is less than 0.05 as shown in Fig. 26. In the presence of hand, the ECC is further reduced as some of the transmitted power is lost in the hand. Hence the two antennas are less correlated in the real case scenario than in free space. The measured ECC in free space is higher than the simulated ECC. This is due to the addition of the DC bias wire resulting in the increase of coupling of RF signal and DC supply lines. As both antennas are provided with the same DC supply to bias the corresponding varactor diode, there will be a leakage of RF energy into one another. This leads to discrepancy in the measured ECC.

VI. CONCLUSIONS

A novel reconfigurable open slot antenna which supports octa-band communication for metal rim integrated smart-phones has been proposed and studied in this paper. A varactor diode has been used to achieve multiple states with the return loss more than 6 dB and total efficiency greater than 50% in free space throughout the bands 698-960 MHz and 1710-2690 MHz. The proposed antenna requires very small ground clearance, thereby achieving miniaturisation, making it suitable for modern smartphones. The proposed antenna has been designed, fabricated and measured. The important parameters of the proposed antenna has been studied thoroughly and also the performance of the antenna in the presence of mobile phone components and the human hand is investigated. Furthermore, the calculated SAR values of this open slot antenna are in compliance with industry standards. In addition, it is possible to realize multiple antennas with high isolation by keeping a copy of the antenna at the upper portion of the system circuit board which is very suitable for MIMO applications for 698-960 MHz and 1710-2690 MHz.

ACKNOWLEDGMENT

The financial support from Huawei Technologies, Shenzhen, China for the project is gratefully acknowledged.

REFERENCES

[1] A. Jensen and Y. Rahmat-Samii, “Performance Analysis of Antennas for Hand-held Transceivers Using FDTD,” *IEEE Trans. Antennas Propag.*, vol.42, no.8, pp. 1106-1113, Aug. 1994.

[2] T. Taga and K. Tsunekawa, “Performance Analysis of a Built-in Planar Inverted-F Antenna for 800 MHz Band Port able Radio Units,” IEEE Journal of Selected Areas in Communications, SAC-5, pp. 921-929, Jun. 1987.

[3] Z. D. Liu, P. S. Hall, and D. Wake, “Dual Frequency Planar Inverted-F Antenna,” *IEEE Trans. Antennas Propag.*, vol.45, no.10, pp. 1451-1458, Oct. 1997.

[4] C. R. Rowell and R. D. Murch, “A Compact PIFA Suitable for Dual-Frequency 900/1800-MHz Operation,” *IEEE Trans. Antennas Propag.*, vol.46, no.4, pp. 596-598, Apr. 1998.

[5] G. F. Pedersen and J. B. Andersen, “Integrated Antennas for Handheld Telephones with Low Absorption,” *Proc. IEEE Vehicular Technology Conference*, Stockholm, Sweden, pp. 1537-1541, Jun. 1994.

[6] K. Kagoshima, K. Tsunekawa, and A. Ando, “Analysis of a Planar Inverted F Antenna Fed by Electromagnetic Coupling,” *Proc. IEEE Antennas Propag. Soc. Int. Symp.*, pp. 1702-1705, Jul. 1992.

[7] Y. J. Cho, S. H. Hwang, and S. O. Park, “A Dual-band Internal Antenna with a Parasitic Patch for Mobile Handsets and the Consideration of the

Handset Case and Battery," *IEEE Antennas Wireless Propag. Lett.,* vol.4, pp. 429-432, Sep. 2005.
[8] P. Ciais, R. Staraj, G. Kossiavas, and C. Luxey, "Compact Internal Multiband Antenna for Mobile Phone and WLAN Standards," *Electron Lett.*, vol.40, no.15, pp. 920-921, Jul. 2004.
[9] I. Szini, C. Di Nallo, and A. Faraone, "The Enhanced Bandwidth Folded Inverted Conformal Antenna (EB FICA) for Multi-band Cellular Handsets," *Proc. IEEE Antennas Propag. Soc. Int. Symp.*, pp. 4697-4700, Jun. 2007.
[10] K. Ishimiya, J.-i. Takada, Zhinong Ying, "Progress of Multi-Band Antenna Technology for Mobile Phone," *Proc. IEEE Antennas Propag. Soc. Int. Symp.*, pp. 1245-1248, Jun. 2007.
[11] Yong-Ling Ban, Yun-Fei Qiang, Zhi Chen, Kai Kang, and Jin-Hong Guo, '' A Dual-Loop Antenna Design for Hepta-Band WWAN/LTE Metal-Rimmed Smartphone Applications'', *IEEE Trans. Antennas Propag.,* vol. 63, no. 1, Jan. 2015.
[12] Y.L. Ban, Peng-Peng Li, C.Y. Desmond Sim and X Chen, "Dual-feed full-metal-case antenna for WWAN/LTE smartphone applications", International Journal of RF and Microwave Computer-Aided Engineering, vol.26, no.7, pp.595-601, 2016.
[13] Y. L. Ban, Li-Wan Zhang, C. Y. Desmond Sim, H. Wang and X Chen, "Hepta-band coupled-fed antenna for WWAN/LTE metal-ring-frame smartphone applications", International Journal of RF and Microwave Computer-Aided Engineering, vol.26, no.7, pp.633-639, 2016.
[14] A. C. K. Mak, C. R. Rowell, R. D. Murch, Chi-Lun Mak, "Reconfigurable Multiband Antenna Designs for Wireless Communication Devices," *IEEE Trans. Antennas Propag.*, vol.55, no.7, pp.1919-1928, Jul. 2007.
[15] R. Hossa, A. Byndas, and M. E. Bialkowski, "Improvement of compact terminal antenna performance by incorporating open-end slots in ground plane," *IEEE Microw. Wireless Compon. Lett.*, vol. 14, no. 6, pp. 283–285, Jun. 2004.
[16] Qingxin Guo, Raj Mittra, Fang Lei, Zengrui Li, Jilong Ju and Joonho Byun, '' Interaction Between Internal Antenna and External Antenna of Mobile Phone and Hand Effect'', *IEEE Trans. Antennas Propag.*, vol. 61, No. 2, Feb. 2013
[17] B. Yuan et al., "Slot antenna for metal-rimmed mobile handsets," *IEEE Antennas Wireless Propag. Lett.,* vol. 11, pp. 1334–1337, Dec. 2012.
[18] Ying Liu, Yan-min Zhou, Gui-feng Liu, and Shu-xi Gong, "Heptaband inverted-f antenna for metal-rimmed mobile phone applications", *IEEE Antennas Wireless Propag. Lett.,* vol. 15, pp.995-999, March. 2016.
[19] Kin-Lu Wong, and Chih-Yu Tsai, Low-profile dual-wideband inverted-T open slot antenna for the LTE/WWAN tablet computer with a metallic frame," IEEE Trans. Antennas Propag., vol. 63, pp. 2879-2886, 2015.
[20] K. L. Wong and L. C. Lee, "Multiband printed monopole slot antenna for WWAN operation in the laptop computer," IEEE Trans. Antennas Propag., vol. 57, no. 2, pp. 324–330, Feb. 2009.
[21] K. L. Wong and W. J. Lin, "WWAN/LTE printed slot antenna for tablet computer application," Microw. Opt. Technol. Lett., vol. 54, pp. 44–49, 2012.
[22] Yong-Ling Ban, Yun-Fei Qiang, Gang Wu, Hanyang Wang and Kin-Lu Wong, "A reconfigurable narrow-frame antenna for LTE/WWAN Metal-Rimmed smartphone applications", *IET Microw. Antennas Propag.*, Apr. 2016.
[23] C. H. Kuo, K. L. Wong, and F. S. Chang, "Internal GSM/DCS dual-band open-loop antenna for laptop application," *Microw. Opt. Technol. Lett.,* vol. 49, no. 3. pp. 680–684, Mar. 2007.
[24] C. C. Lin, R. W. Ziolkowski, "Dual-band 3D magnetic ez antenna," *Microw. Opt. Technol. Lett.*, vol. 52, no. 4. pp. 971–975, Apr. 2010.
[25] C. H. Li, E. Ofli, N. Chavannes, et al., "Effects of hand phantom on mobile phone antenna performance," *IEEE Trans. Antennas Propag.*, vol. 57, no. 9, pp. 2763–2770, Sep. 2009.
[26] M. Berg, M. Sonkki, and E. Salonen, "Experimental study of hand and head effects to mobile phone antenna radiation properties," in *Proc. Eur. Conf. Antennas Propag.*, Mar. 2009, pp. 437–440.
[27] R. Martens, J. Holopainen, E. Safin, J. Ilvonen, and D. Manteuffel, "Optimal dual-antenna design in a small terminal multi-antenna system," *IEEE Antennas Wireless Propag. Lett.,* vol. 12, pp. 1700–1703, Dec. 2013.
[28] Z. Miers, H. Li, and B. K. Lau, "Design of bandwidth enhanced and multiband MIMO antennas using characteristic modes," *IEEE Antennas Wireless Propag. Lett.*, vol. 12, pp. 1696–1699, Nov. 2013.
[29] S Zhang, K Zhao, Z Ying, S He, "Investigation of diagonal antenna-chassis mode in mobile terminal LTE MIMO antennas for bandwidth enhancement," *IEEE Antennas and Propag. Maga.*, vol. 57, no. 2, pp. 24-28, Apr. 2015.
[30] Y. J. Ren, "Ceramic based small LTE MIMO handset antenna," *IEEE Trans. Antennas Propag.*, vol. 61, no. 2, pp. 934–938, Feb. 2013.
[31] K. Zhao, S. Zhang, K. Ishimiya, *et al.*, "Body-insensitive multimode MIMO terminal antenna of double-ring structure," *IEEE Trans. Antennas Propag.*, vol. 63, no. 5, pp. 1925–1936, May. 2015.
[32] W. J. Liao, S. H. Chang, J. T. Yeh, *et al.*, "Compact dual-band WLAN diversity antennas on USB dongle platform," *IEEE Trans. Antennas Propag.*, vol. 62, no. 1, pp. 109–118, Jan. 2014.
[33] Test Plan for Wireless Device Over the-Air Performance. (2016, Jul.), Method of Measurement for Radiated RF Power and Receiver Performance, CTIA certification Program. [online] http://www.ctia.org/docs/default-source/default-document-library/ctia-test-plan-for-wireless-device-over-the-air-performance-ver-3-5-2.pdf

Manoj Stanley received the B.Tech degree in Electronics & Communication from Kerala University, India in 2012. He received his M.Tech degree in Communication Systems from Visvesvaraya National Institute of Technology, India in 2014. He also worked as a lab engineer under CoE at Visvesvaraya National Institute of Technology where he was involved in projects of national importance. He is currently working towards the Ph.D. degree in electrical engineering at the University Of Liverpool, U.K. His research interests include mobile phone antenna design, theory of characteristic modes, MIMO and mm-wave antenna array design for 5G smartphones.

Yi Huang (S'91–M'96–SM'06) received B.Sc. degree in physics from Wuhan University, China, the M.Sc. (Eng.) degree in microwave engineering from NRIET, Nanjing, China, and the D.Phil. degree in communications from the University of Oxford, Oxford, U.K., in 1994.

He has been conducting research in the areas of wireless communications, applied electromagnetics, radar and antennas for the past 25 years. His experience includes 3 years spent with NRIET (China) as a Radar Engineer and various periods with the Universities of Birmingham, Oxford, and Essex, in the U.K., as a member of research staff. He worked as a Research Fellow at British Telecom Labs in 1994, and then joined the Department of Electrical Engineering & Electronics, the University of Liverpool, U.K., as a Faculty member in 1995, where he is now a Full Professor in Wireless Engineering, the Head of High Frequency Engineering Research Group, M.Sc. Programme Director and Deputy Head of Department. He has published over 200 refereed papers in leading international journals and conference proceedings, and is the principal author of the popular book Antennas: from Theory to Practice (Wiley, 2008). He has received many research grants from research councils, government agencies, charity, EU, and industry, acted as a consultant to various companies, and served on a number of national and international technical committees.

Prof. Huang has been an Editor, Associate Editor, or Guest Editor of four of international journals. He has been a keynote/invited speaker and organiser of many conferences and workshops (e.g., IEEE iWAT 2010, WiCom 2006, 2010, and

This article has been accepted for publication in a future issue of this journal, but has not been fully edited. Content may change prior to final publication. Citation information: DOI 10.1109/TAP.2017.2700084, IEEE Transactions on Antennas and Propagation

LAPC2012). He is at present the Editor-in-Chief of Wireless Engineering and Technology, a UK National Rep of European COST-IC1102, an Executive Committee Member of the *IET Electromagnetics PN*, and a Fellow of IET, U.K

Hanyang Wang (SM'03) received the Ph.D. degree from Heriot-Watt University, Edinburgh, U.K., in 1995. He served as a Lecturer and an Associate Professor with Shandong University, Jinan, China, from 1986 to 1991. From 1995 to 1999, he was a Post-Doctoral Research Fellow with the University of Birmingham, Birmingham, U.K., and the University of Essex, Colchester, U.K. From 1999 to 2000, he was with Vector Fields Ltd., Oxford, U.K., as a Software Development and Microwave Engineering Consultant Engineer. He joined Nokia U.K. Ltd., Farnborough, U.K., in 2001, where he was a Mobile Antenna Specialist for 11 years. He joined Huawei Technologies after leaving Nokia, and he is currently the Chief Mobile Antenna Expert and the Head of the Mobile Antenna Technology Division. He is also an Adjunct Professor with the School of Electronics and Information Technology, Sichuan University, Chengdu, China. His current research interests include small antennas for mobile terminals, patch and slotted waveguide antennas and arrays for mobile communications and airborne radars, and numerical methods for the solutions of electromagnetic radiation and scattering problems. He holds over 40 granted and pending US/WO/PCT patents, and he has authored over 80 refereed papers on these topics. He was a recipient of the Title of Nokia Inventor of the Year in 2005 and the Nokia Excellence Award in 2011. He was also a recipient of the Huawei Individual Gold Medal Award in 2012 and the Huawei Team Gold Medal Award in 2013 and 2014, respectively. His patent was ranked number one among 2015 Huawei top ten patent awards. Dr. Wang is a Huawei Fellow, an IET/IEE Fellow, and an IEEE Senior Member. He is an Associate Editor of the IEEE Antennas and Wireless Propagation Letters. He is listed in Marquis Who's Who in the World and the International Biographical Center, Cambridge, U.K.

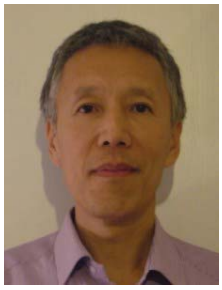

Hai Zhou received a Ph.D degree in 1987 from University of London, where he also carried out his post doctoral work until 1992. He served as a senior lecturer at South Bank University, London before joining Lucent Technologies in 1996 and worked in system engineering for 19 years before moving to Huawei Technologies in 2015 working on OTA (Over-The-Air) test related standards and 5G antennas. He worked on various topics from shaped reflector antenna synthesis, FDTD during his academic years to radio resource management and adaptive antennas in industry, with 18 patents, 14 journal papers and 34 conference papers. One of the papers won the Best Paper Award at the 19th European Microwave Conference in 1989, another received Oliver Lodge premium from IEE as the best paper of the year on Antennas and Propagation in 1991.

Zhihao Tian received the B.Sc. degree in optic information science and technology from National University of Defence Technology (NUDT), Changsha, China, in 2011. He pursued his M.Eng. degree in high power microwave technology from 2011-2013 in NUDT. He is currently working towards the Ph.D. degree in electrical engineering at the University Of Liverpool, U.K.

Qian Xu received the B.Eng. and M.Eng. degrees from the Department of Electronics and Information, Northwestern Polytechnical University, Xi'an, China, in 2007 and 2010, and received the PhD degree in electrical engineering from the University of Liverpool, U.K, in 2016. He is currently an Associate Professor at the College of Electronic and Information Engineering, Nanjing University of Aeronautics and Astronautics, China. He worked as a RF engineer in Nanjing, China in 2011, an Application Engineer at CST Company, Shanghai, China in 2012 and a Research Assistant at the University Of Liverpool, UK in 2016. His research interests include statistical electromagnetics, reverberation chamber, computational electromagnetics, and anechoic chamber.